Journal of Sound and Vibration (2002) **255**(2), 243–259
doi:10.1006/jsvi.2001.4153, available online at http://www.idealibrary.com on IDEAL®

INSTABILITY OF VIBRATION OF A MOVING-TRAIN-AND-RAIL COUPLING SYSTEM

D. Y. Zheng and S. C. Fan

School of Civil and Structural Engineering, Nanyang Technological University, Nanyang Avenue, Singapore 639798, *Singapore. E-mails: cdyzheng@ntu.edu.sg, cfansc@ntu.edu.sg*

(*Received* 24 *November* 2000, *and in final form* 14 *December* 2001)

This paper presents the derivation of the governing equations for the stability of vibration of an integrated system comprising a moving train and the railway track. The train consists of a convoy of articulated two-axle wagons. The equations are applicable to any *arbitrary number* of axles at *arbitrary spacing*. Each axle is modelled as a mass–spring–damper vibration unit. The railway track is an infinitely long Euler beam subjected to an axial compressive force and rests on a visco-elastic foundation. The governing equations for the integrated system are coupled differential equations, which can be transformed to algebraic equations by Fourier and Laplace transforms. Subsequent inverse Fourier transform and contour integration yield the instability equation. Critical parameter is identified. It follows by parametric studies on the instability of vibration due to different train configurations. Illustrative examples for trains having up to 20 wagons or 40 axles are given.

1. INTRODUCTION

The instability of vibration of an integrated system comprising a moving train and the railway track is of great practical importance to the civil and transportation engineering. The instability of vibration is due to the negative damping effect of the coupling system. Excessive vibration due to this negative damping imposes a great danger to the moving train. It may lead to disastrous accident. Amongst the prevailing models for the moving-train-and-rail system, a train is often simulated as an infinitely long chain of evenly spaced oscillators [1–3]. Sometimes even more unrealistically, a train is considered just as a single moving force [4] or mass [5, 6], or a vehicle having a single axle [7, 8]. In this paper, a more realistic model is presented. The train is simulated as a convoy of articulated two-axle wagons. The convoy can consist of an *arbitrary number* of axles at *arbitrary spacing*. In the mathematical model, each axle is converted into a mass–spring–damper vibration unit. The railway track is modelled as an infinitely long Euler beam, which is subjected to an axial compression force and rests on a visco-elastic foundation. The analysis of this integrated system could be rather mathematically involved. In this paper, a not-so-involved method of solution is presented. Firstly based on Newton's second law, the governing differential equations for the integrated system are derived. Secondly, the differential equations are transformed to algebraic equation via the well-developed techniques. The spatial variables go with the Fourier transform while the temporal variables demand the Laplace transform. Hence, the instability equation is obtained and finally solved through inverse Fourier transform and contour integration. The next section shows the detailed derivations, followed by a section on procedures of getting the solution.

0022-460X/02/$35.00

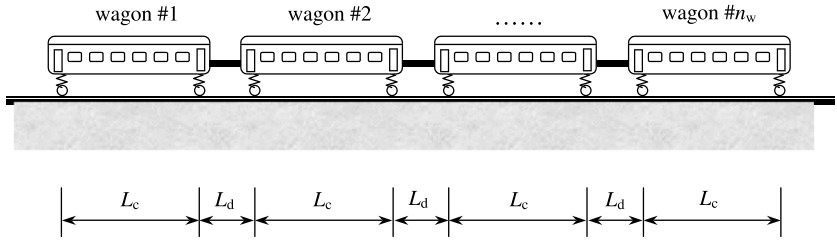

Figure 1. An n_w-wagon train and its axle configuration.

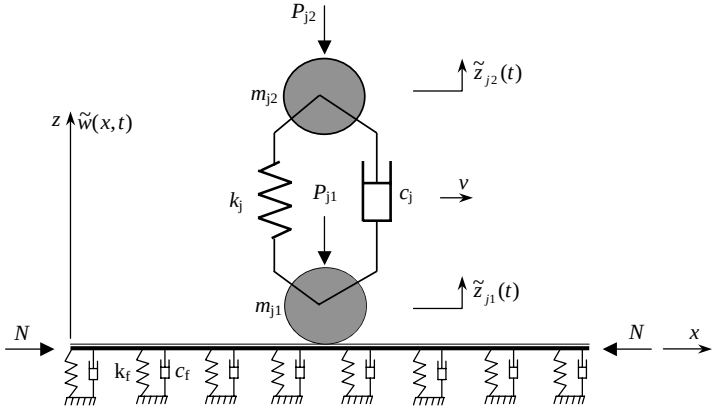

Figure 2. Mathematical model for a typical jth moving axle.

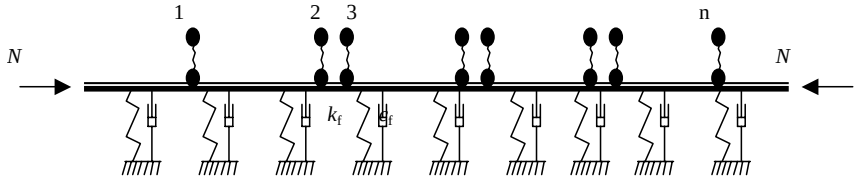

Figure 3. Mechanical model of a train-and-rail on visco-elastic foundation.

Identification of the critical parameter is illustrated. Finally, parametric studies via numerical examples are given.

2. GOVERNING DIFFERENTIAL EQUATIONS

Figure 1 shows a train and its configuration. In the mathematical model, each axle is converted into a mass–spring–damper vibration unit. The model for a typical (jth) axle is illustrated in Figure 2. Figure 3 shows the mechanical model of a train moving atop of the rail, which is simulated as an axially compressed Euler beam resting on visco-elastic foundation. The cross-sectional area of the Euler beam is denoted by A, the second moment of area is I, the mass density is ρ, Young's modulus is E, and the compressive axial force is N. The visco-elastic foundation is characterized by the stiffness k_f and viscosity c_f per unit length. A typical (jth) axle is represented by a two-degrees-of-freedom (d.o.f.) system

comprising an unsprung mass m_{j1} and a sprung mass m_{j2}, which are interconnected by a spring having stiffness k_j and a dashpot of damping coefficient c_j. The unsprung and sprung masses are acted upon, respectively, by vertical forces P_{j1} and P_{j2}, which are derived from the self-weight of the masses. Besides, the axle is assumed always in contact with the rail.

The axles travel horizontally atop of the rail at a velocity v. The general governing equation for the vertical vibration of a rail can be written as

$$\rho A\frac{\partial^2\tilde{w}(x,t)}{\partial t^2}+EI\frac{\partial^4\tilde{w}(x,t)}{\partial x^4}+N\frac{\partial^2\tilde{w}(x,t)}{\partial x^2}=q(x,t), \tag{1}$$

where $\tilde{w}(x,t)$ is the deflection of the rail and $q(x,t)$ is the load intensity acting on the rail at location x and time t. The load intensity $q(x,t)$ comprises the viscous and elastic reactions from the foundation and also the contact force between the axles and the rail. In equation form,

$$q(x,t)=-c_f\frac{\partial\tilde{w}(x,t)}{\partial t}-k_f\tilde{w}(x,t)-\sum_{j=1}^{n}f_j(t)\delta(x-vt-x_j), \tag{2}$$

where x_j denotes the distance between the jth and the first axle, and $\delta(\ldots)$ the Dirac delta function. The contact force $f_i(t)$ is derived from the vertical motion of the jth axle as follows:

$$f_j(t)=P_{j1}+P_{j2}+m_{j1}\frac{\mathrm{d}^2\tilde{z}_{j1}(t)}{\mathrm{d}t^2}+m_{j2}\frac{\mathrm{d}^2\tilde{z}_{j2}(t)}{\mathrm{d}t^2} \tag{3}$$

in which $\tilde{z}_{j1}(t)$ and $\tilde{z}_{j2}(t)$ are, respectively, the vertical displacements of the unsprung and sprung mass with reference to their respective static equilibrium positions. Substituting equation (3) into equation (2), and subsequently the result into equation (1) yield,

$$\begin{aligned}&\rho A\frac{\partial^2\tilde{w}(x,t)}{\partial t^2}+EI\frac{\partial^4\tilde{w}(x,t)}{\partial x^4}+N\frac{\partial^2\tilde{w}(x,t)}{\partial x^2}+c_f\frac{\partial\tilde{w}(x,t)}{\partial t}+k_f\tilde{w}(x,t)\\&=-\sum_{j=1}^{n}\left[P_{j1}+P_{j2}+m_{j1}\frac{\mathrm{d}^2\tilde{z}_{j1}(t)}{\mathrm{d}t^2}+m_{j2}\frac{\mathrm{d}^2\tilde{z}_{j2}(t)}{\mathrm{d}t^2}\right]\delta(x-vt-x_j).\end{aligned} \tag{4}$$

Based on the assumption that the axles are always in contact with the rail, the displacement $\tilde{z}_{j1}(t)$ of the unsprung mass and its first and second derivatives can be written as

$$\tilde{z}_{j1}(t)=\tilde{w}(x,t)|_{x=vt+x_j}, \tag{5}$$

$$\frac{\mathrm{d}\tilde{z}_{j1}(t)}{\mathrm{d}t}=\left[\frac{\partial\tilde{w}(x,t)}{\partial t}+v\frac{\partial\tilde{w}(x,t)}{\partial x}\right]_{x=vt+x_j}, \tag{6}$$

$$\frac{\mathrm{d}^2\tilde{z}_{j1}(t)}{\mathrm{d}t^2}=\left[\frac{\partial^2\tilde{w}(x,t)}{\partial t^2}+2v\frac{\partial^2\tilde{w}(x,t)}{\partial x\partial t}+v^2\frac{\partial^2\tilde{w}(x,t)}{\partial x^2}\right]_{x=vt+x_j}. \tag{7}$$

Substituting equation (7) into equation (4) leads to

$$\begin{aligned}&\rho A\frac{\partial^2\tilde{w}(x,t)}{\partial t^2}+EI\frac{\partial^4\tilde{w}(x,t)}{\partial x^4}+N\frac{\partial^2\tilde{w}(x,t)}{\partial x^2}+c_f\frac{\partial\tilde{w}(x,t)}{\partial t}+k_f\tilde{w}(x,t)\\&=-\sum_{j=1}^{n}\left\{P_{j1}+P_{j2}+m_{j1}\left(\frac{\partial^2\tilde{w}(x,t)}{\partial t^2}+2v\frac{\partial^2\tilde{w}(x,t)}{\partial x\partial t}+v^2\frac{\partial^2\tilde{w}(x,t)}{\partial x^2}\right)_{x=vt+x_j}\right.\\&\qquad\left.+m_{j2}\frac{\mathrm{d}^2\tilde{z}_{j2}(t)}{\mathrm{d}t^2}\right\}\delta(x-vt-x_j).\end{aligned} \tag{8}$$

The equation for the vertical vibration of the sprung mass on the jth axle can be written as

$$m_{j2}\frac{\mathrm{d}^2\tilde{z}_{j2}(t)}{\mathrm{d}t^2}+c_j\frac{\mathrm{d}\tilde{z}_{j2}(t)}{\mathrm{d}t}+k_j\tilde{z}_{j2}(t)=k_j\tilde{z}_{j1}(t)+c_j\frac{\mathrm{d}\tilde{z}_{j1}(t)}{\mathrm{d}t}. \tag{9}$$

Substituting equations (5) and (6) into equation (9) leads to

$$m_{j2}\frac{\mathrm{d}^2\tilde{z}_{j2}(t)}{\mathrm{d}t^2}+c_j\frac{\mathrm{d}\tilde{z}_{j2}(t)}{\mathrm{d}t}+k_j\tilde{z}_{j2}(t)=k_j\tilde{w}(x,t)|_{x=vt+x_j}+c_j\left[\frac{\partial\tilde{w}(x,t)}{\partial t}+v\frac{\partial\tilde{w}(x,t)}{\partial x}\right]_{x=vt+x_j} \tag{10}$$

To render the governing differential equations dimensionless, the following dimensionless parameters are introduced:

time: $$\tau=t/(\sqrt{\rho A/k_f}), \tag{11}$$

length: $$\{y, y_j, \bar{w}(y,\tau), \bar{z}_{j2}(\tau)\}=\{x, x_j, \tilde{w}(x,t), \tilde{z}_{j2}(t)\}/(\sqrt[4]{4EI/k_f}), \tag{12–15}$$

mass: $$\{M_{j1}, M_{j2}\}=\{m_{j1}, m_{j2}\}/(\rho A\sqrt[4]{4EI/k_f}), \tag{16, 17}$$

force: $$\{T, F_{j1}, F_{j2}\}=\{N, P_{j1}, P_{j2}\}/(\sqrt{4EIk_f}), \tag{18–20}$$

velocity: $$\alpha=v/(\sqrt[4]{4EIk_f/\rho^2A^2}), \tag{21}$$

foundation damping: $$\mu_f=c_f/(\sqrt{\rho Ak_f}), \tag{22}$$

axle damping: $$\mu_j=c_j/(\sqrt[4]{4EI\rho^2A^2k_f}), \tag{23}$$

axle stiffness: $$K_j=k_j/(\sqrt[4]{4EIk_f^3}). \tag{24}$$

Using these dimensionless parameters, equations (8) and (10) can be rewritten as

$$\begin{aligned}&\frac{\partial^2\bar{w}(y,\tau)}{\partial\tau^2}+\mu_f\frac{\partial\bar{w}(y,\tau)}{\partial\tau}+\frac{1}{4}\frac{\partial^4\bar{w}(y,\tau)}{\partial y^4}+T\frac{\partial^2\bar{w}(y,\tau)}{\partial y^2}+\bar{w}(y,\tau)\\&\quad=-\sum_{j=1}^{n}\left\{F_{j1}+F_{j2}+M_{j1}\left(\frac{\partial^2\bar{w}(y,\tau)}{\partial\tau^2}+2\alpha\frac{\partial^2\bar{w}(y,\tau)}{\partial y\partial\tau}+\alpha^2\frac{\partial^2\bar{w}(y,\tau)}{\partial y^2}\right)_{y=\alpha\tau+y_j}\right.\\&\qquad\left.+M_{j2}\frac{d^2\bar{z}_2(\tau)}{\mathrm{d}\tau^2}\right\}\delta(y-\alpha\tau-y_j),\end{aligned} \tag{25}$$

$$M_{j2}\frac{d^2\bar{z}_{j2}(\tau)}{\mathrm{d}\tau^2}+\mu_j\frac{\mathrm{d}\bar{z}_{j2}(\tau)}{\mathrm{d}\tau}+K_j\bar{z}_{j2}(\tau)=\left[K_j\bar{w}(y,\tau)+\mu_j\left(\frac{\partial\bar{w}(y,\tau)}{\partial\tau}+\alpha\frac{\partial\bar{w}(y,\tau)}{\partial y}\right)\right]_{y=\alpha\tau+y_j}. \tag{26}$$

For the sake of convenience, a moving reference system in terms of the temporal and spatial variables (θ and ξ) is adopted, i.e.,

$$\theta=\tau, \qquad \xi=y-\alpha\tau. \tag{27, 28}$$

The corresponding displacement functions $w(\xi,\theta)$ and $z_{j2}(\theta)$, respectively, for the rail and sprung mass on the jth axle can therefore be rewritten as

$$\bar{w}(y,\tau)=\bar{w}(\xi+\alpha\theta,\theta)=w(\xi,\theta); \qquad \bar{z}_{j2}(\tau)=\bar{z}_{j2}(\theta)=z_{j2}(\theta). \tag{29, 30}$$

By the chain rule,

$$\frac{\partial^n}{\partial y^n} = \frac{\partial^n}{\partial \xi^n}, \quad \frac{\partial^n}{\partial \tau^n} = \left(\frac{\partial}{\partial \theta} - \alpha \frac{\partial}{\partial \xi}\right)^n, \quad \frac{\partial^{m+n}}{\partial y^m \partial \tau^n} = \frac{\partial^m}{\partial \xi^m}\left(\frac{\partial}{\partial \theta} - \alpha \frac{\partial}{\partial \xi}\right)^n \tag{31–33}$$

equations (25) and (26), respectively, become

$$\frac{\partial^2 w(\xi,\theta)}{\partial \theta^2} - 2\alpha \frac{\partial^2 w(\xi,\theta)}{\partial \xi \partial \theta} + (T+\alpha^2)\frac{\partial^2 w(\xi,\theta)}{\partial \xi^2} + \frac{1}{4}\frac{\partial^4 w(\xi,\theta)}{\partial \xi^4} + \mu_f \frac{\partial w(\xi,\theta)}{\partial \theta}$$

$$- \mu_f \alpha \frac{\partial w(\xi,\theta)}{\partial \xi} + w(\xi,\theta)$$

$$= -\sum_{j=1}^{n}\left\{F_{j1} + F_{j2} + \left[M_{j1}\frac{\partial^2 w(\xi,\theta)}{\partial \theta^2}\right]_{\xi=y_j} + M_{j2}\frac{\mathrm{d}^2 z_{j2}(\theta)}{\mathrm{d}\theta^2}\right\}\delta(\xi - y_j), \tag{34}$$

$$M_{j2}\frac{d^2 z_{j2}(\theta)}{\mathrm{d}\theta^2} + \mu_j \frac{\mathrm{d}z_{j2}(\theta)}{\mathrm{d}\theta} + K_j z_{j2}(\theta) = \left[K_j w(\xi,\theta) + \mu_j \frac{\partial w(\xi,\theta)}{\partial \theta}\right]_{\xi=y_j} \quad (j = 1, 2, \ldots, n) \tag{35}$$

which are the governing differential equations for the moving-train-and-rail vibration system. It is worth noting that the second term in equation (34) represents the damping of the coupling system. The sign is negative. It is the cause of the instability.

3. SOLUTIONS BY INTEGRAL TRANSFORM

The techniques of Laplace and Fourier transform [9] are employed to solve the governing differential equations. The Laplace transformation is carried out with respect to θ, while the Fourier transformation is carried out with respect to ξ. The transformed functions $w(\xi, \theta)$ and $z_{j2}(\theta)$ are, respectively:

$$\bar{W}(\xi, s) = L[w(\xi,\theta)] = \int_0^\infty w(\xi,\theta)\mathrm{e}^{-s\theta}\,\mathrm{d}\theta, \tag{36}$$

$$W(\omega, s) = F[\bar{W}(\xi, s)] = \int_{-\infty}^{\infty} \bar{W}(\xi, \mathrm{s})\mathrm{e}^{-\mathrm{i}\omega\xi}\,\mathrm{d}\xi, \tag{37}$$

$$Z_{j2}(s) = L[z_{j2}(\theta)] = \int_0^\infty z_{j2}(\theta)\mathrm{e}^{-\mathrm{s}\theta}\,\mathrm{d}\theta. \tag{38}$$

Applying the Laplace transform to equations (34) and (35) yields

$$s^2\bar{W}(\xi,s) + \mu_f s\bar{W}(\xi,s) - 2\alpha s\frac{\partial \bar{W}(\xi,s)}{\partial \xi} + (T+\alpha^2)\frac{\partial^2 \bar{W}(\xi,s)}{\partial \xi^2} + \frac{1}{4}\frac{\partial^4 \bar{W}(\xi,s)}{\partial \xi^4}$$

$$- \mu_f \alpha \frac{\partial \bar{W}(\xi,s)}{\partial \xi} + \bar{W}(\xi,s) = -\sum_{j=1}^{n}\left[\frac{F_{j1}+F_{j2}}{s} + M_{j1}s^2\bar{W}(y_j,s) + M_{j2}s^2 Z_{j2}(s)\right]\delta(\xi - y_j), \tag{39}$$

$$M_{j2}s^2 Z_{j2}(s) + \mu_j \mathrm{s} Z_{j2}(\mathrm{s}) + \mathrm{K}_j Z_{j2}(s) = K_j\bar{W}(y_j,s) + \mu_j s\bar{W}(y_j,s). \tag{40}$$

The transformed $Z_{j2}(s)$ can, therefore, be solved from equation (40) such that,

$$Z_{j2}(s) = \frac{(\mu_j s + K_j)\bar{W}(y_j, s)}{M_{j2}s^2 + \mu_j s + K_j}. \tag{41}$$

Substituting equation (41) into equation (39) yields

$$s^2\bar{W}(\xi, s) + \mu_f s\bar{W}(\xi, s) - 2\alpha s\frac{\partial\bar{W}(\xi, s)}{\partial\xi} + (T + \alpha^2)\frac{\partial^2\bar{W}(\xi, s)}{\partial\xi^2} + \frac{1}{4}\frac{\partial^4\bar{W}(\xi, s)}{\partial\xi^4}$$
$$- \mu_f\alpha\frac{\partial\bar{W}(\xi, s)}{\partial\xi} + \bar{W}(\xi, s) = -\sum_{j=1}^{n}\left[\frac{F_{j1} + F_{j2}}{s} + Q_j(s)\,\bar{W}(y_j, s)\right]\delta(\xi - y_j), \tag{42}$$

where $Q_j(s)$ is given by

$$Q_j(s) = M_{j1}s^2 + \frac{M_{j2}s^2(\mu_j s + K_j)}{M_{j2}s^2 + \mu_j s + K_j}. \tag{43}$$

By further applying Fourier transform to equation (42), we have

$$D(\omega, s)\,W(\omega, s) = -\sum_{j=1}^{n}\left[\frac{F_{j1} + F_{j2}}{s} + Q_j(s)\,\bar{W}(y_j, s)\right]e^{-i\omega y_j}, \tag{44}$$

where

$$D(\omega, s) = s^2 + \mu_f s - 2i\alpha s\omega + \frac{\omega^4}{4} - (T + \alpha^2)\omega^2 - i\mu_f\alpha\omega + 1. \tag{45}$$

Hence, the transformed $W(\omega, s)$ can be obtained from equation (44) such that

$$W(\omega, s) = -\frac{1}{D(\omega, s)}\sum_{j=1}^{n}\left[\frac{F_{j1} + F_{j2}}{s} + Q_j(s)\bar{W}(y_j, s)\right]e^{-i\omega y_j}. \tag{46}$$

Performing an inverse Fourier transform on equation (46), we have

$$\bar{W}(\xi, s) = -\sum_{j=1}^{n}\left[\frac{F_{j1} + F_{j2}}{s} + Q_j(s)\bar{W}(y_j, s)\right]\frac{1}{2\pi}\int_{-\infty}^{\infty}\frac{e^{i\omega(\xi - y_j)}d\omega}{D(\omega, s)}. \tag{47}$$

The transformed $\bar{W}(y_j, s)$ $(j = 1, 2, \ldots, n)$ can be obtained from equation (47) by putting $\xi = y_l$ $(l = 1, 2, \ldots, n)$ such that

$$\bar{W}(y_l, s) = -\sum_{j=1}^{n}\left[\frac{F_{j1} + F_{j2}}{s} + Q_j(s)\bar{W}(y_j, s)\right]\frac{1}{2\pi}\int_{-\infty}^{\infty}\frac{e^{i\omega(y_l - y_j)}d\omega}{D(\omega, s)} \quad (l = 1, 2, \ldots, n). \tag{48}$$

By denoting

$$H_{lj}(s) = \left(\frac{1}{2\pi}\int_{-\infty}^{\infty}\frac{e^{i\omega(y_l - y_j)}d\omega}{D(\omega, s)}\right)^{-1} \quad (l, j = 1, 2, \ldots, n) \tag{49}$$

equation (48) can be rewritten as

$$\sum_{j=1}^{n}H_{lj}^{-1}(s)Q_j(s)\bar{W}(y_j, s) + \bar{W}(y_l, s) = -\sum_{j=1}^{n}H_{lj}^{-1}(s)\frac{F_{j1} + F_{j2}}{s} \quad (l = 1, 2, \ldots, n). \tag{50}$$

The solution to equation (50) can be written as

$$\bar{W}(y_j, s) = \frac{b_j(s)}{|\mathbf{A}(s)|} \quad (j = 1, 2, \ldots, n), \tag{51}$$

where

$$\mathbf{A}(s) = \begin{bmatrix} \dfrac{Q_1 + H_{11}}{H_{11}} & \dfrac{Q_2}{H_{12}} & \cdots & \dfrac{Q_n}{H_{1n}} \\ \dfrac{Q_1}{H_{21}} & \dfrac{Q_2 + H_{22}}{H_{22}} & \cdots & \dfrac{Q_n}{H_{2n}} \\ \cdots & \cdots & \cdots & \cdots \\ \dfrac{Q_1}{H_{n1}} & \dfrac{Q_2}{H_{n2}} & \cdots & \dfrac{Q_n + H_{nn}}{H_{nn}} \end{bmatrix}. \tag{52}$$

Hence, substituting equation (51) into equations (47) and (41), respectively, yields:

$$\bar{W}(\xi, s) = -\sum_{j=1}^{n} \left[\frac{F_{j1} + F_{j2}}{s} + Q_j(s) \frac{b_j(s)}{|\mathbf{A}(s)|} \right] \frac{1}{2\pi} \int_{-\infty}^{\infty} \frac{e^{i\omega(\xi - y_j)}\, d\omega}{D(\omega, s)}$$

$$= -\sum_{j=1}^{n} \frac{F_{j1} + F_{j2}}{s} \frac{1}{2\pi} \int_{-\infty}^{\infty} \frac{e^{i\omega(\xi - y_j)}\, d\omega}{D(\omega, s)} - \sum_{j=1}^{n} \frac{Q_j(s) b_j(s)}{|\mathbf{A}(s)|} \frac{1}{2\pi} \int_{-\infty}^{\infty} \frac{e^{i\omega(\xi - y_j)}\, d\omega}{D(\omega, s)} \tag{53}$$

and

$$Z_{j2}(s) = \frac{(\mu_j s + K_j)}{M_{j2} s^2 + \mu_j s + K_j} \frac{b_j(s)}{|\mathbf{A}(s)|} \quad (j = 1, 2, \ldots, n). \tag{54}$$

4. INSTABILITY ANALYSIS

4.1. INSTABILITY ANALYSIS—IDENTIFICATION OF CRITICAL PARAMETER

Equation (53) is deliberately written as a sum of two terms. The first represents the response of the rail due to the moving forces only ($M_{j1} = M_{j2} = 0$), while the second is the response due to the train–rail interaction. It is worth noting that the second term has the same poles as those in equation (54) describing the vibration of the train, i.e., $\Delta(s) = |\mathbf{A}(s)| = 0$. The function $\Delta(s)$ can have a pole such that $s = a + ib$, with $a > 0$. It means that the rail's displacements (equation (53)) and the train's vibrations (equation (54)) are growing exponentially with time. In other words, the system becomes unstable. The roots of the equation,

$$\Delta(s) = |\mathbf{A}(s)| = 0 \tag{55}$$

determine the complex eigenfrequencies of vibrations of the system. The primary concern is whether the root of equation (55) has a positive real part such that it lies on the right half of the s-plane. Amongst all the physical parameters that determine the location of the root in the s-plane, the total mass M of the convoy is the most influential. Against this background, equation (55) is rewritten as follows:

$$\Delta(M, s) = |\mathbf{A}(M, s)| = 0. \tag{56}$$

When the total mass M equals a critical value M^*, the root of equation (56) will lie on the imaginary axis of the s-plane. As such, the critical equation to determine those roots is

$$\Delta(M^*, \mathrm{i}\Omega^*) = |\mathbf{A}(M^*, \mathrm{i}\Omega^*)| = 0. \tag{57}$$

- *For a single-axle convoy*:
  If the convoy comprises only one axle, the critical equation (55) can be written as

$$\Delta(s) = Q_1(s) + H_{11}(s) = 0. \tag{58}$$

Equation (58) has the same form as that in both references [6, 8]. The critical parameter M^* can then be solved using the D-decomposition technique.

- *For a convoy comprising arbitrary number of axles*:
  If the convoy comprises an arbitrary number of axles, it is difficult to use the D-decomposition technique to find the critical parameter M^*. To overcome these difficulties, the problem can be converted to non-linear algebraic equations as follows:

$$\begin{cases} f_1(M, \Omega) = \mathrm{Re}|\mathbf{A}(M, \mathrm{i}\Omega)| = 0, \\ f_2(M, \Omega) = \mathrm{Im}|\mathbf{A}(M, \mathrm{i}\Omega)| = 0. \end{cases} \tag{59}$$

By solving equation (59), we can easily obtain M^* and Ω^*.

4.2. EVALUATION OF $H_{lj}(\mathrm{i}\Omega)$

To compute the matrix $\mathbf{A}(M, \mathrm{i}\Omega)$, the term $H_{lj}(\mathrm{i}\Omega)$ needs to be evaluated first. From equation (49) we have

$$H_{lj}(\mathrm{i}\Omega) = \left(\frac{1}{2\pi} \int_{-\infty}^{\infty} \frac{\mathrm{e}^{\mathrm{i}\omega(y_l - y_j)} \mathrm{d}\omega}{D(\omega, \mathrm{i}\Omega)} \right)^{-1}. \tag{60}$$

By using the contour integration method, equation (60) can be rewritten in terms of the residues of poles in the upper complex s-plane as follows:

$$H_{lj}(\mathrm{i}\Omega) = \left[4i \sum_{\omega_n \in U} \frac{(\omega - \omega_n)\mathrm{e}^{\mathrm{i}\omega(y_l - y_j)}}{(\omega - \omega_1)(\omega - \omega_2)(\omega - \omega_3)(\omega - \omega_4)} \bigg|_{\omega = \omega_n} \right]^{-1} \quad (l \geqslant j), \tag{61a}$$

$$H_{lj}(\mathrm{i}\Omega) = \left[4i \sum_{\omega_n \in U} \frac{(\omega - \omega_n)\mathrm{e}^{\mathrm{i}\omega(y_j - y_l)}}{(\omega - \omega_1)(\omega - \omega_2)(\omega - \omega_3)(\omega - \omega_4)} \bigg|_{\omega = \omega_n} \right]^{-1} \quad (l < j) \tag{61b}$$

in which ω_1, ω_2, ω_3, ω_4 in equation (61a) are the roots of the algebraic equation $D(\omega, \mathrm{i}\Omega) = 0$; and ω_1, ω_2, ω_3, ω_4 in equation (61b) are the roots of the algebraic equation $D(-\omega, \mathrm{i}\Omega) = 0$.

5. STEADY STATE RESPONSE AND STATIC RESPONSE OF THE RAIL

5.1. STEADY STATE RESPONSE

Assuming that the steady state vibration $w^{ss}(\xi)$ of the rail exists, we have [9]

$$w^{ss}(\xi) = \lim_{s \to 0} s\bar{W}(\xi, s). \tag{62}$$

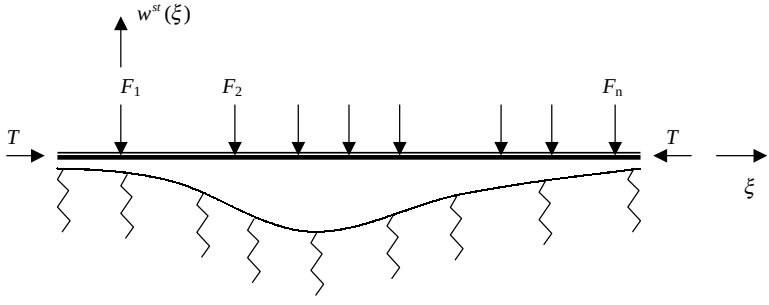

Figure 4. Static response of a rail subjected to an axial compression force T and vertical forces $F_1 = F_{11} + F_{21}$; $F_2 = F_{21} + F_{22}$; ..., $F_n = F_{n1} + F_{n2}$.

Substituting equation (53) into equation (62) yields

$$w^{ss}(\xi) = -\lim_{s\to 0} s\sum_{j=1}^{n}\left[\frac{F_{j1}+F_{j2}}{s} + Q_j(s)\bar{W}(y_j, s)\right]\frac{1}{2\pi}\int_{-\infty}^{\infty}\frac{e^{i\omega(\xi-y_j)}}{D(\omega, s)}\,d\omega. \tag{63}$$

Noticing that $Q_j(0) = 0$, we can simplify equation (63) into

$$w^{ss}(\xi) = -\sum_{j=1}^{n}\frac{F_{j1}+F_{j2}}{2\pi}\int_{-\infty}^{\infty}\frac{e^{i\omega(\xi-y_j)}\,d\omega}{D(\omega, 0)}. \tag{64}$$

By contour integration, the integral in equation (64) can be expressed as

$$\frac{1}{2\pi}\int_{-\infty}^{\infty}\frac{e^{i\omega(\xi-y_j)}\,d\omega}{D(\omega, 0)} = 4i\sum_{\omega_n\in U}\left.\frac{(\omega-\omega_n)e^{i\omega(\xi-y_j)}}{(\omega-\omega_1)(\omega-\omega_2)(\omega-\omega_3)(\omega-\omega_4)}\right|_{\omega=\omega_n}, \quad (\xi \geqslant y_j) \tag{65a}$$

$$\frac{1}{2\pi}\int_{-\infty}^{\infty}\frac{e^{i\omega(\xi-y_j)}\,d\omega}{D(\omega, 0)} = 4i\sum_{\omega_n\in U}\left.\frac{(\omega-\omega_n)e^{i\omega(y_j-\xi)}}{(\omega-\omega_1)(\omega-\omega_2)(\omega-\omega_3)(\omega-\omega_4)}\right|_{\omega=\omega_n}, \quad (\xi < y_j) \tag{65b}$$

in which $\omega_1, \omega_2, \omega_3, \omega_4$ in equation (65a) are the roots of the algebraic equation $D(\omega, 0) = 0$; and $\omega_1, \omega_2, \omega_3, \omega_4$ in equation (65b) are the roots of the algebraic equation $D(-\omega, 0) = 0$.

5.2. STATIC RESPONSE

Figure 4 shows the static response of the railway track under axial compression force T and vertical loads $F_1, F_2, \ldots, F_n$. The governing equation is

$$\frac{1}{4}\frac{d^4w^{st}(\xi)}{d\xi^4} + T\frac{d^2w^{st}(\xi)}{d\xi^2} + w^{st}(\xi) = -\sum_{j=1}^{n}(F_{j1}+F_{j2})\delta(\xi-y_j). \tag{66}$$

Applying Fourier transform to both sides of equation (66) leads to

$$W^{st}(\omega) = -\frac{1}{D_1(\omega)}\sum_{j=1}^{n}(F_{j1}+F_{j2})e^{-i\omega y_j}, \tag{67}$$

where

$$D_1(\omega) = \tfrac{1}{4}\omega^4 - T\omega^2 + 1. \tag{68}$$

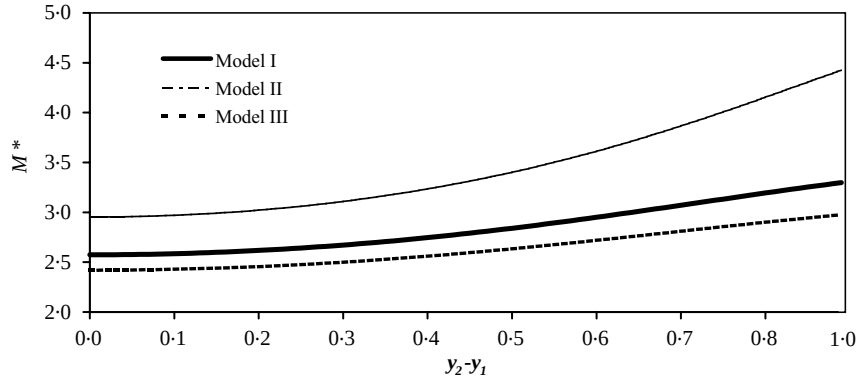

Figure 5. Effect of distance between two axles on the critical total mass parameter M^* ($\mu_f = 0{\cdot}001$, $\alpha = 0{\cdot}9$, $T = 0{\cdot}5$; Model I: $r_{m1} = 0{\cdot}2$, $r_{m2} = 0{\cdot}8$; Model II: $r_{m1} = 1{\cdot}0$, $r_{m2} = 0{\cdot}0$; Model III: $r_{m1} = 0{\cdot}0$, $r_{m2} = 1{\cdot}0$; $K_v = 1{\cdot}0$, $\mu_v = 1{\cdot}0$ where applicable).

Performing inverse Fourier transform on both sides of equation (67), we can obtain the static response as follows:

$$w^{st}(\xi) = -\sum_{j=1}^{n} \frac{F_{j1} + F_{j2}}{2\pi} \int_{-\infty}^{\infty} \frac{e^{i\omega(\xi - y_j)}\, d\omega}{D_1(\omega)}. \tag{69}$$

The integral in equation (69) can be computed via contour integration:

$$\frac{1}{2\pi}\int_{-\infty}^{\infty} \frac{e^{i\omega(\xi - y_j)}\, d\omega}{D_1(\omega)} = 4i \sum_{\omega_n \in U} \left. \frac{(\omega - \omega_n) e^{i\omega(\xi - y_j)}}{(\omega - \omega_1)(\omega - \omega_2)(\omega - \omega_3)(\omega - \omega_4)} \right|_{\omega = \omega_n} \quad (\xi \geqslant y_j) \tag{70a}$$

$$\frac{1}{2\pi}\int_{-\infty}^{\infty} \frac{e^{i\omega(\xi - y_j)}\, d\omega}{D_1(\omega)} = 4i \sum_{\omega_n \in U} \left. \frac{(\omega - \omega_n) e^{i\omega(y_j - \xi)}}{(\omega - \omega_1)(\omega - \omega_2)(\omega - \omega_3)(\omega - \omega_4)} \right|_{\omega = \omega_n} \quad (\xi < y_j) \tag{70b}$$

in which ω_1, ω_2, ω_3, ω_4 in equation (70a) are the roots of the algebraic equation $D_1(\omega) = 0$; and ω_1, ω_2, ω_3, ω_4 in equation (70b) are the roots of the algebraic equation $D_1(-\omega) = 0$.

6. PARAMETRIC STUDIES VIA NUMERICAL EXAMPLES

6.1. EFFECT OF SPACING BETWEEN TWO AXLES ON THE TOTAL CRITICAL MASS M^*

To study the effect of the spacing between two axles, a simple two-axle wagon is first considered. The foundation has a very small damping ($\mu_f = 0{\cdot}001$) and the rail is subjected to an axial compression load equal to half of the buckling load ($T = 0{\cdot}5$). A relatively high velocity ($\alpha = 0{\cdot}9$) is considered. It represents a usual working velocity of 294 km/h of a high-speed train with the rail and foundation parameters [10]: $E = 210$ GPa, $A = 6{\cdot}742\text{E-}3\ \text{m}^2$, $\mu = 0{\cdot}3$, $I = 2{\cdot}231\text{E-}5\ \text{m}^4$, $\rho = 7800\ \text{kg/m}^3$ and $k_f = 10\ \text{kN/m}^2$. Two axles have the same stiffness and damping characteristic parameters: $K_v = 1{\cdot}0$, $\mu_v = 1{\cdot}0$. But three kinds of axle model are investigated: Model I consists of both unsprung and sprung masses ($r_{m1} = 0{\cdot}2$, $r_{m2} = 0{\cdot}8$); Model II has unsprung mass only ($r_{m1} = 1{\cdot}0$, $r_{m2} = 0{\cdot}0$); while Model III has sprung mass only ($r_{m1} = 0{\cdot}0$, $r_{m2} = 1{\cdot}0$). The critical total mass parameter M^* is plotted in Figure 5 against the spacing between two axles [dimensionless $(y_2 - y_1)$, actual $0 - 6{\cdot}58$ m]. It can be seen that the vibration system can bear higher critical mass

TABLE 1

Critical total mass of a high–speed moving convoy ($T = 0{\cdot}5$, $\mu_f = 0{\cdot}001$, $\alpha = 0{\cdot}9$; $l_d = 0{\cdot}7$, $l_c = 2{\cdot}1$)

No. of wagons (N_w)	No. of axles (n)	M^*		
		Model I $r_{m1} = 0{\cdot}2$, $r_{m2} = 0{\cdot}8$	Model II $r_{m1} = 1{\cdot}0$, $r_{m2} = 0{\cdot}0$	Model III $r_{m1} = 0{\cdot}0$, $r_{m2} = 1{\cdot}0$
—	1	2·2919	2·9529	2·0794
1	2	3·4017	4·4171	3·0858
2	4	4·0813	4·8195	3·8027
3	6	4·6102	5·2367	4·3517
4	8	4·9999	5·5360	4·7646
5	10	5·3565	5·8378	5·1369
6	12	5·7397	6·1952	5·5267
7	14	6·1194	6·5582	5·9105
8	16	6·4849	6·9110	6·2793
9	18	6·8666	7·2879	6·6612
10	20	7·2691	7·6921	7·0615
11	22	7·6772	8·1040	7·4661
12	24	8·0986	8·5332	7·8827
13	26	8·5499	8·9978	8·3268
14	28	9·0275	9·4936	8·7950
15	30	9·5306	10·0195	9·2864
16	32	10·0764	10·5963	9·8172
17	34	10·6792	11·2418	10·3998
18	36	11·3479	11·9699	11·0413
19	38	12·1142	12·8271	11·7682
20	40	13·0478	13·9286	12·6361

parameter M^*, if the two axles are separated further apart. Besides, Model I comprising both unsprung and sprung masses has a critical mass parameter M^* always lower than that in Model II, but always higher than that in Model III. It is worth noting that when the spacing between two axles drops to zero, that is equivalent to a combined single axle, the computed critical mass parameters M^* are found exactly the same as those in references [6–8].

6.2. EFFECT OF NUMBER OF AXELS ON THE CRITICAL TOTAL MASS M^* OF CONVOYS

The parameters chosen are similar to those used in Section 6.1. The foundation has a very small damping ($\mu_f = 0{\cdot}001$) and the rail is subjected to an axial compression load equal to half of the buckling load ($T = 0{\cdot}5$). A relatively high velocity ($\alpha = 0{\cdot}9$) is considered. The axle configuration of the train is dimensionless $l_d = 0{\cdot}7$, $l_c = 2{\cdot}1$ (actual $L_d = 4{\cdot}61$ m, $L_c = 13{\cdot}82$ m). All axles have the same stiffness and damping characteristic parameters, $K_v = 1{\cdot}0$, $\mu_v = 1{\cdot}0$. The critical total masses for convoys comprising up to 20 wagons (40 axles) are computed and shown in Table 1 and Figure 6. Again, three kinds of axle models are investigated: Model I consists of both unsprung and sprung masses ($r_{m1} = 0{\cdot}2$, $r_{m2} = 0{\cdot}8$); Model II has unsprung mass only ($r_{m1} = 1{\cdot}0$, $r_{m2} = 0{\cdot}0$); while Model III has sprung mass only ($r_{m1} = 0{\cdot}0$, $r_{m2} = 1{\cdot}0$). It can be seen from Figure 6 that a train comprising more wagons (or axles) bears higher critical masses. Once more, it is worth noting that when

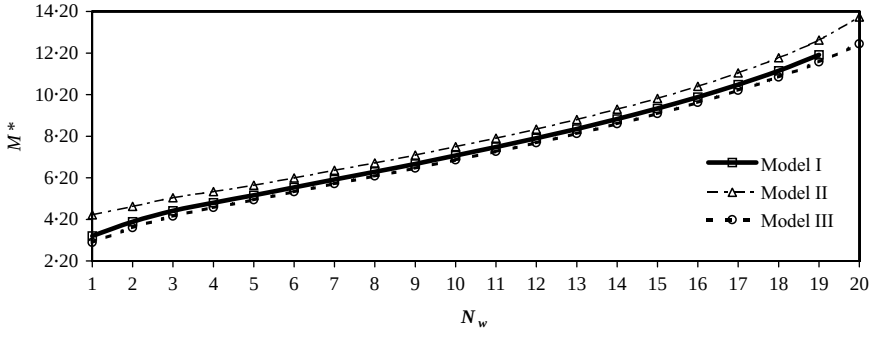

Figure 6. Dependance of critical total mass parameter M^* on the number of wagons ($\mu_f = 0{\cdot}001$, $T = 0{\cdot}5$, $\alpha = 0{\cdot}9$; $l_d = 0{\cdot}7$, $l_c = 2{\cdot}1$, $K_v = 1{\cdot}0$, $\mu_v = 1{\cdot}0$).

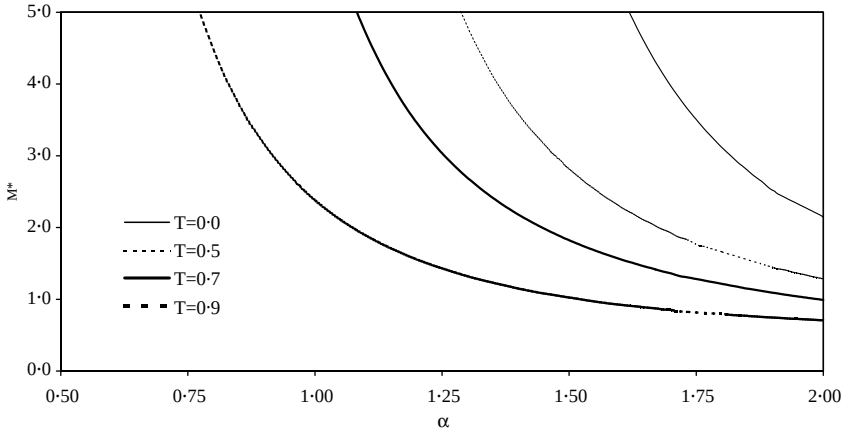

Figure 7. Dependence of critical total mass parameter M^* on velocity parameter of a 20-wagon train under different axial compression forces ($\mu_f = 0{\cdot}001$; $K_v = 2{\cdot}0$, $\mu_v = 2{\cdot}5$, $r_{m1} = 0{\cdot}2$, $r_{m2} = 0{\cdot}8$, $l_d = 0{\cdot}7$, $l_c = 2{\cdot}1$).

the train comprises only one axle, the computed results agree exactly with those in references [6–8].

6.3. EFFECT OF TRAIN VELOCITY AND RAIL'S COMPRESSIVE FORCE ON THE CRITICAL TOTAL MASS M^*

For the sake of parametric studies, the foundation's damping remains unchanged ($\mu_f = 0{\cdot}001$). Four cases of axial compressive force ($T = 0{\cdot}0$, $0{\cdot}5$, $0{\cdot}7$ and $0{\cdot}9$ respectively) in the rail are investigated. The train has 20 wagons (or 40 axles). The configuration of the axles is dimensionless $l_d = 0{\cdot}7$, $l_c = 2{\cdot}1$ (actual $L_d = 4{\cdot}61$ m, $L_c = 13{\cdot}82$ m). All axles have the same stiffness, damping and masses characteristic parameters, $K_v = 2{\cdot}0$, $\mu_v = 2{\cdot}5$, $r_{m1} = 0{\cdot}2$, $r_{m2} = 0{\cdot}8$. The critical total mass parameters M^* are plotted against the velocities α in Figure 7. The velocity α ranges from $0{\cdot}7$ to $2{\cdot}0$. Assuming that the rail and foundation have the same parameters as those in section 6.1, it is equivalent to a high speed of 228 km/h to a yet-to-achieve ultra-high speed of 653 km/h. It can be seen that the existence of axial compression force will lead to significantly lower values of critical total mass parameter M^*.

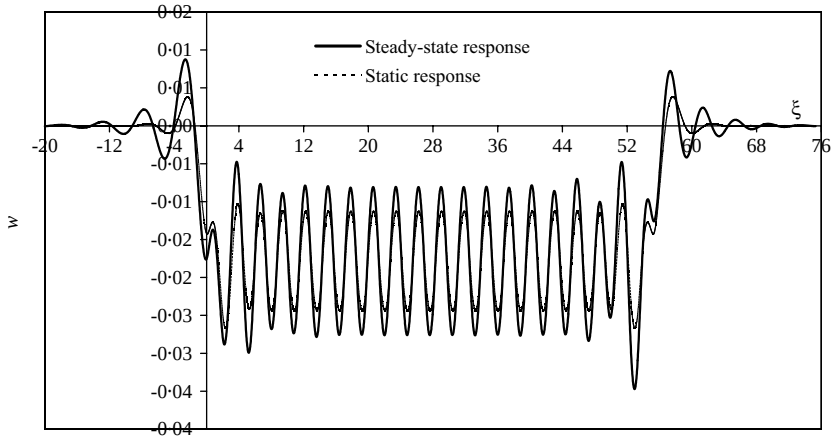

Figure 8. Steady state and static responses of rail to a moving 20-wagon train for $\mu_f = 0{\cdot}25$, $\alpha = 0{\cdot}5$, $T = 0{\cdot}7$; $F = 1{\cdot}0$, $l_d = 0{\cdot}7$, $l_c = 2{\cdot}1$ ($D_m = 1{\cdot}301$).

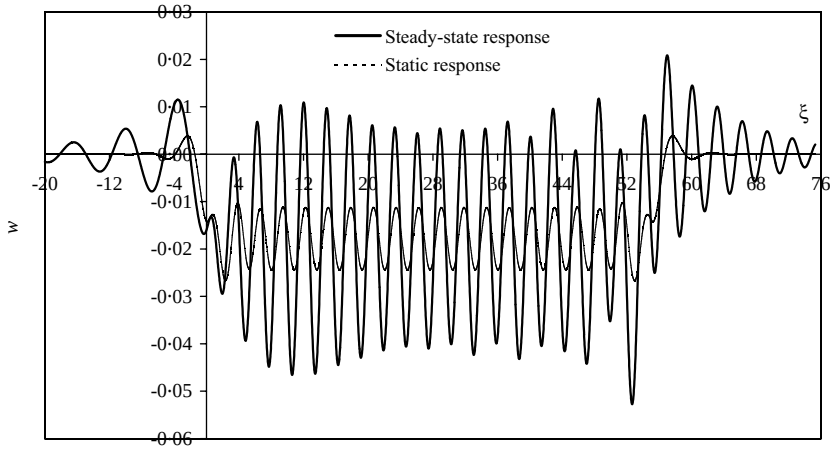

Figure 9. Steady state and static responses of rail to a moving 20-wagon train for $\mu_f = 0{\cdot}25$, $\alpha = 0{\cdot}75$, $T = 0{\cdot}7$; $F = 1{\cdot}0$, $l_d = 0{\cdot}7$, $l_c = 2{\cdot}1$ ($D_m = 1{\cdot}977$).

In fact, a value of 1·2 is generally high enough for the parameter α to cover most cases encountered in engineering.

6.4. FFECTS OF TRAIN-SPEED ON DYNAMIC MAGNIFICATION FACTOR

In this section, the static and dynamic reponses of the rail are investigated, in particular the dynamic magnification factors (D_m). The parameters chosen are: foundation damping $\mu_f = 0{\cdot}25$, axial compressive force in rail $T = 0{\cdot}7$ (equivalent to 303 kN assuming that the rail and foundation have the same parameters as those in section 6.1), train configuration having $l_d = 0{\cdot}7$ and $l_c = 2{\cdot}1$, and axle characteristics being $r_{m1} = 0{\cdot}2$, $r_{m2} = 0{\cdot}8$, $K_v = 2{\cdot}0$, $\mu_v = 2{\cdot}5$. The responses of the rail to a 20-wagon train moving at three different speeds — $\alpha = 0{\cdot}5$, 0·75 and 1·5 (equivalent to 163, 245, 490 km/h) are investigated. The results are in Figures 8–10. It is interesting to note that the dynamic magnification factors for these three

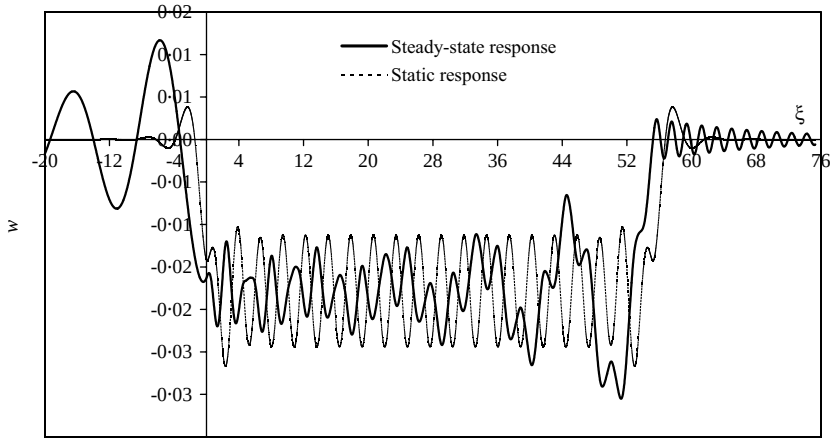

Figure 10. Steady state and static responses of rail to a moving 20-wagon train for $\mu_f = 0{\cdot}25$, $\alpha = 1{\cdot}5$, $T = 0{\cdot}7$; $F = 1{\cdot}0$, $l_d = 0{\cdot}7$, $l_c = 2{\cdot}1$ ($D_m = 1{\cdot}143$).

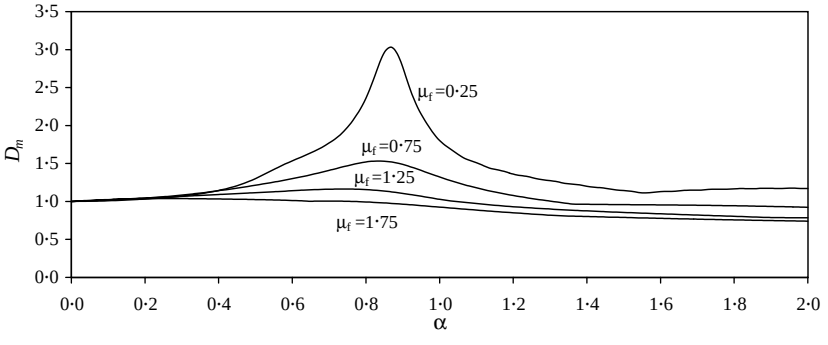

Figure 11. Dependence of dynamic magnification factor on velocity parameter of a 20-wagon train moving atop a rail (axial force $T = 0{\cdot}7$).

speeds are 1·301, 1·977 and 1·143 respectively. Again, a value of 1·2 is generally high enough for the parameter α to cover most cases encountered in engineering.

6.5. FFECTS OF FOUNDATION DAMPING ON DYNAMIC MAGNIFICATION FACTOR

The same 20-wagon train but moving along a rail having a compressive force of $T = 0{\cdot}7$ was investigated. Four different foundation dampings are considered: $\mu_f = 0{\cdot}25$, $0{\cdot}75$, $1{\cdot}25$ and $1{\cdot}75$ respectively. The effects of foundation damping on the dynamic magnification factors (D_m) are shown in Figure 11.

6.6. EFFECTS OF RAIL'S AXIAL COMPRESSIVE FORCE ON THE CRITICAL FOUNDATION DAMPING

The same 20-wagon train is used. The effects of rail's axial compressive force (T) on the critical foundation damping (μ_f^{cr}) are investigated. The results are shown in Figure 12. It can

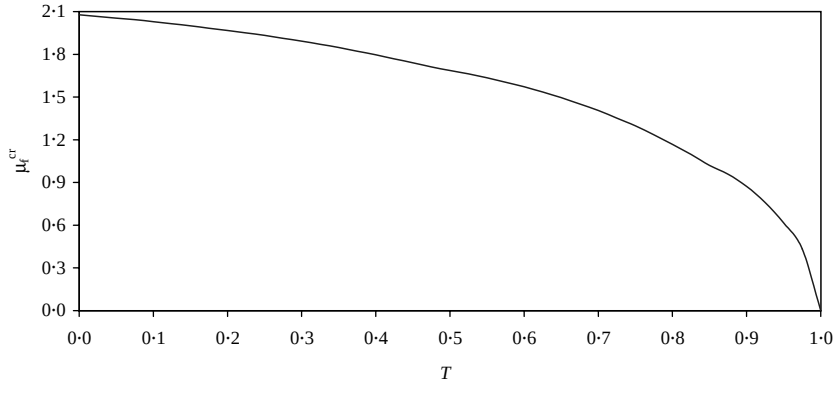

Figure 12. Critical foundation damping of a 20-wagon train–and–rail system.

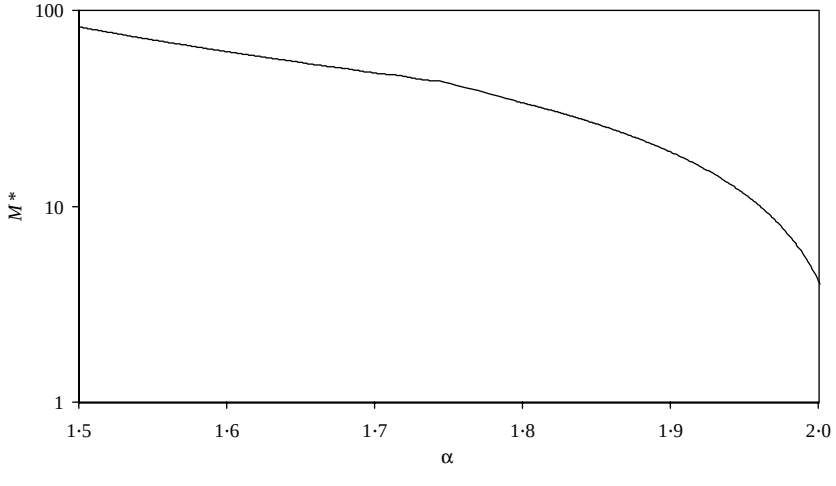

Figure 13. Critical total mass parameter M^* of a 20-wagon train moving atop a rail on foundation of over damping ($T = 0{\cdot}7$, $\mu_f = 1{\cdot}5^*\mu_f{}^{cr} = 2{\cdot}109$).

be seen that higher axial compression force (T) results in lower critical foundation damping (μ_f^{cr}).

6.7. CRITICAL TOTAL MASS PARAMETER M^* OF A TRAIN–RAIL SYSTEM WITH OVER-DAMPED FOUNDATION

The same 20-wagon train is used. The rail is subjected to an axial compressive force $T = 0{\cdot}7$ and the system is assumed having a critical foundation damping $\mu_f^{cr} = 1{\cdot}406$. Effect of over-damped foundation ($\mu_f = 1{\cdot}5\mu_f^{cr}$) on the critical total mass parameter M^* is investigated. The results are shown in Figure 13. It is worth noting that, contrary to the conventional belief, even in the case of over damping ($\mu_f = 1{\cdot}5\mu_f^{cr}$), the stability of the integrated system is not guranteed although the resonance is suppressed. These findings concur to those reported in refrences [6–8], in which a single axle was considered.

On the other hand, it is worth noting that the specific train speed α depends on the specific value $c_{min} = \sqrt[4]{4\,EI\,k_f/\rho^2 A^2}$, which is the minimum propagation speed of elastic

wave in the railway track. The value of c_{min} can be as high as up to 1930 km/h [4] for a normal track foundation. That speed is definitely beyond the reach of current technology. However, cautions should be taken in the case of weak track foundation (i.e., small k_f), in which the value of c_{min} could be as low as the normal working speed of a train. Therefore, the foundation stiffness (k_f) plays a very important role in the determination of the instability of the system. Besides, it should be noted that it is the response of the integrated system. It is not for a fixed point on the railway track. In other words, the instability is "built up" from the continuous oscillatory interaction between the moving train and the rail. As long as the physical foundation situation and the train configuration prevails, when the train travels at the critical speed, instability of the system could occur. It means that the response can go "without bound". It is due to the existence of negative damping of the coupled dynamic system.

7. CONCLUSIONS

The governing differential equations for a train–rail–foundation coupled system are derived. The equation for the instability of vibration is obtained via Fourier and Laplace transforms. The total mass is identified as the critical parameter. Various physical variables were found influencing the critical total mass to different extent. Amongst them, the effects due to axle spacing, total number of axles, rail's compressive force, train velocity, foundation damping were investigated. Increasing the spacing between axles generally leads to higher critical mass. It is same for more axles. On the opposite, higher compressive force in the rail or higher train velocity leads to lower total critical mass. But higher foundation damping allows higher total critical mass. Besides, no clear relationship can be observed between the train speed and the dynamic magnification factor. It is so for the foundation damping and the dynamic magnification factor. Furthermore, the governing equations reveal the existence of negative damping in the coupled train–rail–foundation system. A stiffer foundation will diminish the negative damping and hence reduce the danger of instability. On the other hand, it was found that, contrary to common belief, higher foundation damping (or over-damping) alone cannot eliminate the occurrence of instability. It is because the negative damping not only depends on the foundation damping but also the train speed.

REFERENCES

1. L. FRYBA 1972 *Vibration of Solids and Structures under Moving Loads*. Groningen, The Netherlands: Noordhoff International.
2. R. BOGACZ 1983 *Ingenieur Archiv* **53**, 243–255. On dynamics and stability of continuous systems subjected to a distributed moving load.
3. R. BOGACZ, S. NOWAKOWSKI and K. POPP 1986 *Acta Mechanica* **61**, 117–127. On the stability of a Timoshenko beam on an elastic foundation under a moving spring–mass system.
4. A. D. KERR 1972 *International Journal for Mechanical Science* **14**, 71–78. The continuously supported rail subjected to an axial force and a moving load.
5. G. G. DENISOV, E. K. KUGASHEVA and V. V. NOVIKOV 1985 *Journal of Applied Mathematics and Mechanics* **49**, 533–537. On the problem of the stability of one-dimensional unbounded elastic systems.
6. A. V. METRIKINE and H. A. DIETERMAN 1997 *Journal of Sound and Vibration* **201**, 567–576. Instability of vibrations of a mass moving uniformly along an axially compressed beam on a viscoelastic foundation.
7. D. Y. ZHENG 1999 *Ph.D. Thesis, The University of Hong Kong, Hong Kong*. Vibration and Stability Analysis of Plate-type Structures Under Moving Loads by Analytical and Numerical Methods.

8. D. Y. ZHENG, F. T. K. AU and Y. K. CHEUNG 2000 *American Society of Civil Engineers Journal of Engineering Mechanics* **126**, 1141–1147. Vibration of vehicle on compressed rail on viscoelastic foundation.
9. J. Y. LIU, D. Y. ZHENG and Z. J. MEI 1995 *Practical Integral Transforms in Engineering* (in Chinese) China: Huazhong University of Science and Technology Press.
10. W. H. WILLIAM 1982 *Railroad Engineering*. New York: John Wiley & Sons, second edition.

APPENDIX A: NOMENCLATURE

A	cross-sectional area of a rail (m^2)
$\mathbf{A}(s)$	characteristic matrix of a moving-train-and-rail system
c_f	viscosity per unit length of a foundation ($N\,s/m^2$)
c_j $(j = 1, 2, \ldots, n)$	damping coefficient of the jth axle ($N\,s/m$)
E	Young's modulus for rail (N/m^2)
$f_j(t)$ $(j = 1, 2, \ldots, n)$	contact force between the jth axle and the rail (N)
$\{F_{j1}, F_{j2}\}$	dimensionless vertical force acting on the jth axle
I	second moment of area of cross-section of a rail (m^4)
k_f	stiffness per unit length of a foundation (N/m^2)
k_j $(j = 1, 2, \ldots, n)$	spring stiffness of the jth axle (N/m)
K_j	dimensionless stiffness of the jth axle
Kv	dimensionless stiffness of all identical axles in a train
m_{j1}, m_{j2} $(j = 1, 2, \ldots, n)$	unsprung and sprung masses, respectively, on the jth axle (kg)
$\{M_{j1}, M_{j2}\}$	dimensionless unsprung and sprung mass on the jth axle
M^*	critical total mass parameter of a train
n	number of axles in a train
N	compressive axial force exerted on the rail (N)
N_w	number of wagons in a train
P_{j1}, P_{j2} $(j = 1, 2, \ldots, n)$	vertical forces acting on the unsprung and sprung masses, respectively, on the jth axle (N)
r_{m1}	mass ratio of $m_1/(m_1 + m_2)$
r_{m2}	mass ratio of $m_2/(m_1 + m_2)$
T	dimensionless axial compression force
$\tilde{w}(x, t)$	deflection of a rail at location x and time t (m)
$\bar{w}(y, \tau)$	dimensionless deflection of a rail
$w(\xi, \theta)$	dimensionless deflection of a rail in the moving reference co-ordinate system
$\bar{W}(\xi, s)$	Laplace transform of $w(\xi, \theta)$
$W(\omega, s)$	Fourier transform of $\bar{W}(\xi, s)$
x_j $(j = 1, 2, \ldots, n)$	distance between the j^{th} and the first axle (m)
y	dimensionless co-ordinate
y_j	dimensionless distance between the jth and the first axle
$\tilde{z}_{j1}(t), \tilde{z}_{j2}(t)$	vertical displacements of the unsprung and sprung masses, respectively, on the jth axle at time t (m)
$\bar{z}_{j2}(\tau)$	dimensionless displacement of the sprung mass on the jth axle
$z_{j2}(\theta)$	dimensionless displacement of the sprung mass on the jth axle in the moving reference co-ordinate system
$Z_{j2}(s)$	Laplace transform of $z_{j2}(\theta)$
ρ	mass density of a rail (kg/m^3)
δ	Dirac delta function
τ	dimensionless time
α	dimensionless velocity of a train
μ	the Poisson ratio for rail
μ_j	dimensionless damping of the jth axle
μ_v	dimensionless damping of all identical axles in a train
θ	$\theta = \tau$
ξ	moving reference co-ordinate: $\xi = y - \alpha\tau$
$\Delta(s)$	characteristic determinant: $\Delta(s) = \lvert\mathbf{A}(s)\rvert$